NIPPON STEEL TECHNICAL REPORT No. 126 MARCH 2021

Technical Report

Development of Austenitic Steel with Reduced Amount of Nickel and Molybdenum for Hydrogen Use

Masaharu HATANO* Kazuhisa MATUMOTO
Mitsuki SUGEOI Kenji HATTORI

Abstract

We summarized the results of the alloy design of austenitic steel with a reduced amount of Ni and Mo (STH2) for hydrogen use and the material properties of the STH™2 steel sheet. The alloy design of STH2 was Ni equivalent (Sanga's equation ≥30.2) by adding N and Cu to the basic composition (15Cr-9Mn+Ni) to obtain hydrogen gaseous embrittlement resistance at −40°C. The addition of N and Cu enhanced the γ phase stability and suppressed the localization of strain. The hydrogen gaseous embrittlement resistance has good correlation with the γ phase stability (Sanga's equation), and in addition to Ni, N and Cu were effective elements for the hydrogen gaseous embrittlement resistance. The STH2 steel sheet (Ni equivalent 30.5) has both high strength and compatibility with hydrogen gaseous embrittlement resistance.

1. Introduction

In partnership with Nippon Steel Corporation (ex-Nippon Steel & Sumitomo Metal Corporation), Nippon Steel Stainless Steel Corporation participated in a project of the New Energy and Industrial Technology Development Organization (NEDO, an independent administrative institution), and promoted the R&D of the stainless steel used in the high pressure hydrogen gaseous environment.[1–3] SUS316L (17.5Cr-12−14Ni-2Mo) and/or SUS316 that contain more than 12% Ni are representative stainless steels that are less susceptible to the influence of high pressure hydrogen gas. In these stainless steels, as compared with SUS304 (18Cr-8Ni), the transformation from the austenite phase (γ) to the martensite phase (α') by a plastic deformation-like tensile test is suppressed. The hydrogen gaseous embrittlement of stainless steel is gauged by correlating it with the stability of the austenite (γ) phase.[1–3] Recently, in the austenitic stainless steel, the influence of defective microstructural factors pertaining to the lamination defect, epsilon (ε) phase, and atom vacancy lattice defect on the hydrogen gaseous embrittlement has been clarified through microstructure analysis using the positron annihilation method and/or radiation X-ray diffraction.[4–6]

Currently, the operating condition of steel materials of a hydrogen station is in the range of −40 to 250°C, 20 to 82 MPa of hydrogen gas, and the use of SUS316L and SUS316 is provided as an exemplified standard.[7,8] The stability of the γ phase is pursued by the Ni equivalent equation (Hirayama's equation): 12.6C + 0.35Si + 1.05 Mn + Ni + 0.65Cr + 0.98Mo. Nippon Steel Stainless Steel has commercialized the heavy plate and the sheet products of SUS316L (316L-HNi) of which the aforementioned Ni equivalent was enhanced to 28.5 or above to comply with the exemplified standard provided for the high pressure hydrogen gaseous environment. Furthermore, in the aforementioned NEDO project, we have proposed austenitic stainless steel with reduced Nickel and Molybdenum (hereinafter referred to as austenitic steel with reduced Ni and Mo) (STH2) for hydrogen use that has applicability and compatible high strength for use in the hydrogen gaseous environment.[3,9]

Against this background, Nippon Steel Stainless Steel has developed austenitic steel with reduced Ni and Mo STH™2[*1] wherein the rare metals such as Ni and Mo are reduced. This article describes the concept of the material design for hydrogen use and the principal result of our research and development pertaining to the alloy design of STH2.[3,10] Finally, we introduce the various properties of STH2 steel plate actually produced for the test based on the result of

[*1] STH stands for Stainless Steel with Twinning Induced Plasticity for Hydrogen Energy Systems, and is a registered trademark of Nippon Steel Stainless Steel Corporation.

* Chief Researcher, Dr. Eng., Function Creation Research & Development Div., Research & Development Center, Nippon Steel Stainless Steel Corporation 3434 Ooaza-shimata, Hikari City, Yamaguchi Pref. 743-8550

this R&D.

2. Concept of Material Design for Hydrogen Use

The 0.2% proof stress of SUS316L is relatively small with respect to the structural design standard, and is disadvantageous in further reducing the weight of high hydrogen pressure equipment and/or enhancing the operating pressure thereof. To date, hydrogen gaseous embrittlement has been evaluated in various high strength stainless steels. In the tensile strength test conducted in high pressure hydrogen gas, in SUS630 of the martensitic stainless steel, brittle fracture appearance is observed on lath martensite,[11] and in SUS 329J4L of the ferritic-austenitic duplex stainless steel, brittle fracture appearance is observed mainly in the ferrite phase.[12] In either case, the crystal structure of body-centered-cubic (bbc) of martensite and/or ferrite is suggested to cause the embrittlement. On the other hand, although the TYPE205 of the austenitic stainless steel (17.2Cr-14.6Mn-1.3Ni-0.37N) wherein Ni is replaced by Mn, and N is added has high strength, and the γ phase is stabilized, it is readily embrittled by hydrogen gas.[13] From our research result, we confirmed that the hydrogen gaseous embrittlement of SUS304 is not caused just by the formation of deformation-induced martensitic structure (α' phase), but also has a strong correlation with the plastic deformation of the γ phase proper, and is attributed to the localization of strain by hydrogen.[4, 6] Based on this, we considered that the key to gaining excellent hydrogen gaseous embrittlement resistance is the material design that provides the highly deformation-stable γ phase, does not readily allow the formation of the α' phase, and is controllable to form a deformation microstructure that suppresses strain localization even when strength is enhanced.

3. Alloy Design of STH2

3.1 Enhancement of strength and deformation microstructure control

The austenitic steel with reduced Ni and Mo was selected as a guideline for the alloy design of STH2, and a chemical composition was studied that compatibly realizes: (1) enhancement of strength from the level of SUS316L and (2) deformation microstructure that suppresses the localization of strain. Specifically, Cr-Mn-Ni steel with the chemical composition as shown in Table 1 was vacuum-smelted, and 0.2% proof stress and the deformation microstructure were evaluated. In this study, Mn, N, and Cu were considered as solid-solving elements to enhance γ phase stability. As the index to indicate γ phase stability of a material, the Ni equivalent equation that includes coefficients of N and Cu (Sanga's equation[14]): Ni+0.72Cr+0.88Mo+1.11Mn−0.27Si+0.53Cu+12.93C+7.55N was used. The Ni equivalent of the prepared test material was in the range of 27.5 to 31.5.

Figure 1 shows the relationship between the alloying elements and 0.2% proof strength of austenitic steel with reduced Ni and Mo. 0.2% proof stress was measured by the JIS 13 B tensile strength test with specimens of 2 mm thick cold-rolled and annealed sheets with crystal grain size adjusted to GS No. 8. The measured 0.2% proof stress was analyzed by multiple regression analysis with respect to the total amount of Cr, Mn, Ni, N, and Cu, and the coefficient of the respective element was pursued. Although the amount of C was not intentionally changed, to take into account the dispersion of carbon in smelting, proof strength was analyzed by multiple regression analysis with respect to C+N. The multiple regression equation of 0.2% proof stress has a large coefficient of the interstitial type solid-solving element N, and further, Cr and Mn also interacted as strengthening elements. On the other hand, Ni and Cu have negative value coefficients, and are estimated as having small interaction with respect to enhancing strength. The effect of the interaction of the respective element was generally similar to that in the experimental result reported about the TYPE300 of the austenitic stainless steel[15] that conventionally employs Ni as the major γ phase stabilizing element.

Table 1 Chemical compositions of test materials

(mass%)

C	Si	Mn	Cr	Ni	Cu	N	Ni_{eq}
0.06	0.5	8.0–12.0	14.0–16.0	4.0–7.5	0–3.0	0.03–0.25	27.5–31.5

Ni_{eq}=Ni+0.72Cr+0.88Mo+1.11Mn−0.27Si+0.53Cu+12.93C+7.55N

Figure 2 shows examples of analysis of deformation microstructures of austenitic steel with reduced Ni and Mo by the electron backscatter diffraction method (EBSD), which indicate the interactive effect of the added N and Cu. Test pieces were taken from: a) base steel (15Cr-9Mn-6Ni), b) N-added steel (0.1%N), and c) Cu-added steel (1%Cu). The microstructure analysis by the EBSD method was conducted for the tensile test pieces of JIS 13 B provided with uniform elongation of 30% at room temperature in atmospheric air. In the phase-MAPs, the green color regions correspond to the γ phase (fcc) and the red color regions correspond to the α' phase (bcc). In the base steel, about 10% of the α' phase was formed. The N-added steel and the Cu-added steel consist of the γ single phase alone. In the KAM-MAP that shows the extent of misorientation, when observed with focus on the deformation microstructure of the γ phase, in the base steel, as compared with the N-added steel and the Cu-added steel, misorientation becomes larger (green to yellow) in the local sections in the vicinity of crystal grain boundaries and/or within crystal grains, and localization of strain is observed. Namely, in the austenitic steel with reduced Ni and Mo, the addition of N and/or Cu has the effects of enhancing γ phase stability and suppressing the localization of strain.

Thus, the basic composition of the austenitic steel with reduced Ni and Mo was determined as 15Cr-9Mn+Ni+N+Cu with Ni equivalent ≥29.0 to realize the deformation microstructure capable of achieving 0.2% proof stress exceeding 300 N/mm^2 and of suppressing the strain localization.

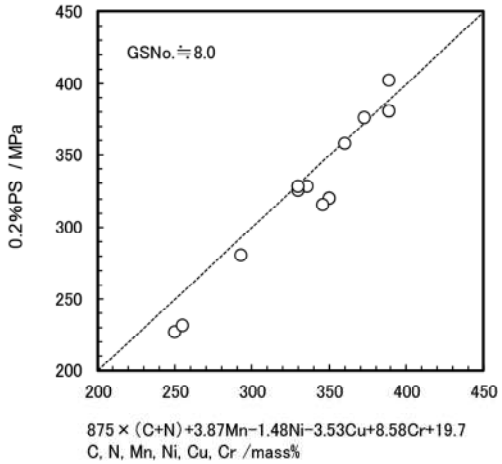

Fig. 1 Relationship between alloying elements and 0.2% proof stress of γ steels reduced amount of nickel and molybdenum

3.2 Hydrogen gaseous embrittlement resistance at −40°C

Conventionally, the hydrogen gaseous embrittlement of austenitic stainless steel becomes apparent not at room temperature but at a low temperature around −40 to −70°C.[16] This phenomenon is explained by the relationship between the fraction of the α' phase and the hydrogen diffusion coefficient. In the alloy design of STH2, it was intended to obtain the hydrogen gaseous resistance at −40°C based on the aforementioned basic composition. For concrete evaluation, 30 to 45 kg of 13 types of steel in which Ni equivalent was varied in the range of 29.0 to 31.5 by adding Ni, N, and Cu within the range specified in Table 1 were vacuum-smelted and prepared. The vacuum-smelted materials were hot-forged and hot-rolled to 15 mm thick plates, and were solution-treated at 1 100°C for 4 min, and then water-quenched. Round bar test pieces 3 mm in diameter in the parallel section with a length of 20 mm in the rolling direction were taken from the solution-treated materials. The slow strain rate tension test (SSRT) was conducted at the $5.0\times10^{-5}s^{-1}$ strain rate at −40°C in atmospheric air and 70 $MPaH_2$.[7]

Figure 3 shows the examples of side views of the fractured test pieces after SSRT. In the top left, the ratio value of the α' phase (amount of ferrite) measured by a ferrite meter is shown. All test pieces fractured in atmospheric air exhibit cup and corn type fracture mode, and the α' phase ratio decreases to 2.8% from 28.2% along with the increase of Ni equivalent from 29.0 to 30.7. In the Ni equivalent range from 29.0 to 29.6, the fractured test pieces in 70 $MPaH_2$ exhibit a decrease of elongation as compared with those in atmospheric air, and side cracks as shown by the arrows in the photo are observed. The fractured test pieces with Ni equivalent of 30.2 to 30.7 are free of such side cracks, and exhibit the same fracture mode as with those of the test pieces tested in atmospheric air. The phase ratios of α' of these fractured test pieces hardly change from those of the test pieces tested in atmospheric air. In **Fig. 4**, the fracture surfaces of the test pieces shown in Fig. 3 are shown. Test pieces tested in atmospheric air show dimpled ductile fracture surfaces, and about 80% of the reduction of area. Test pieces with Ni equivalent of 29.0 to 29.6 and tested in 70 $MPaH_2$ exhibit pseudo cleavage fracture,[1–3] and the reduction of area drops to 35 to 40%. With Ni equivalent of 30.2 to 30.7, pseudo cleavage fracture does not appear, and the ductile fracture and the reduction of area almost equal to those of the test pieces tested in atmospheric air appear.

The above result reveals that the hydrogen gaseous embrittlement resistance at −40°C is obtained by the austenitic steel with re-

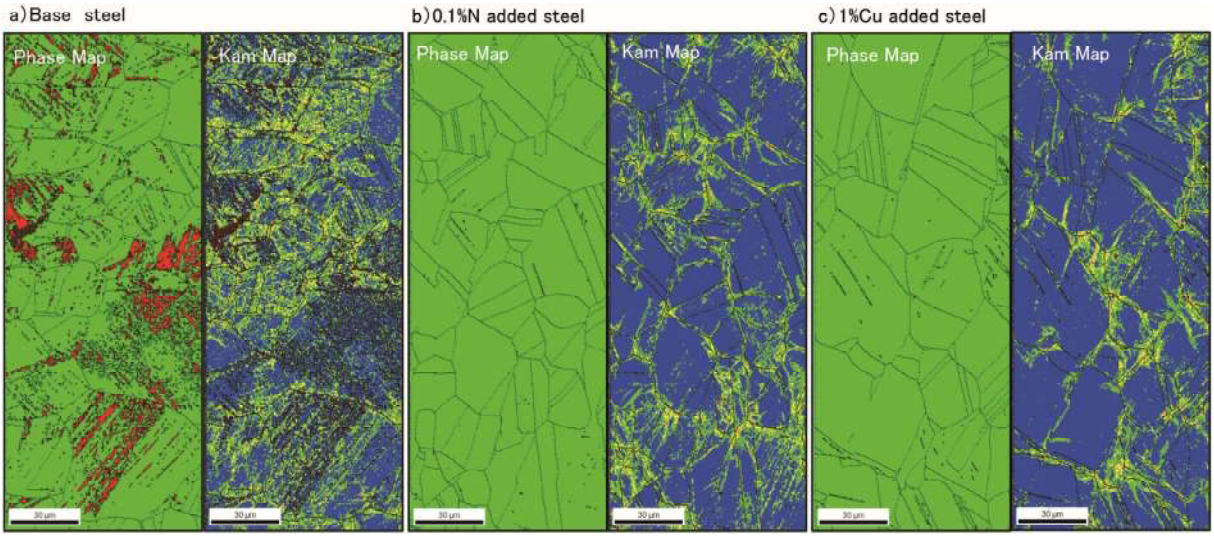

Fig. 2 Analysis of deformation structure of γ steels reduced amount of nickel and molybdenum by EBSD method

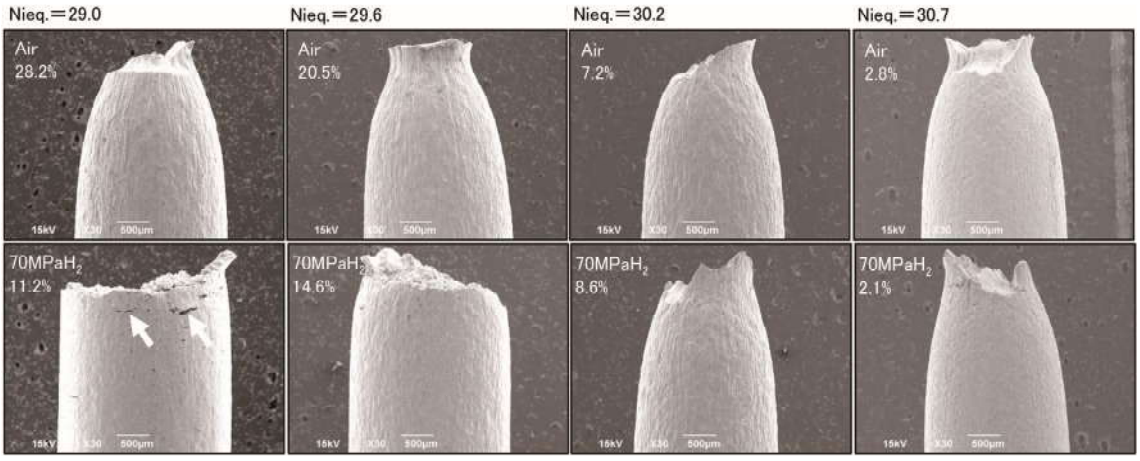

Fig. 3 Side view of fractured specimens after SSRT in gaseous hydrogen at 70 MPa and in air at −40°C

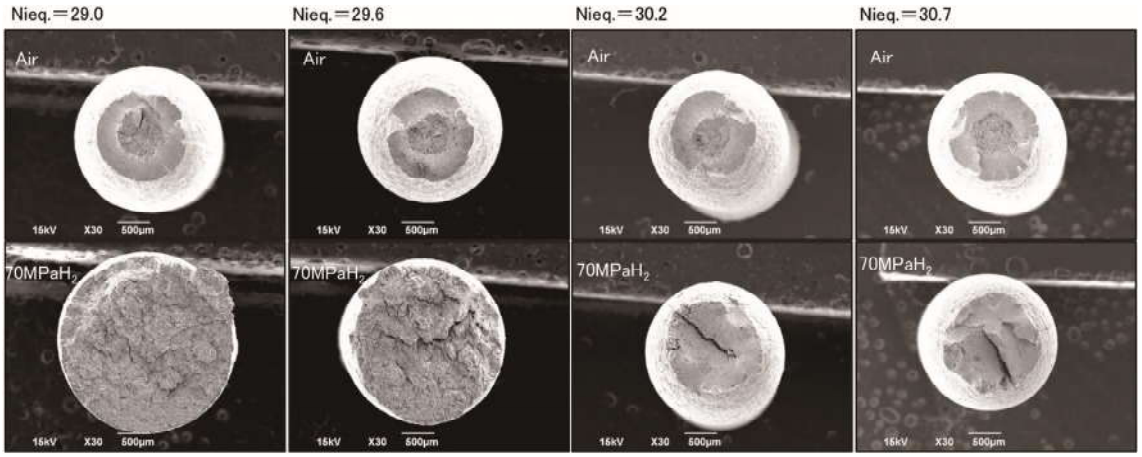

Fig. 4 Fracture surface of the specimens after SSRT in gaseous hydrogen at 70 MPa and in air at −40°C

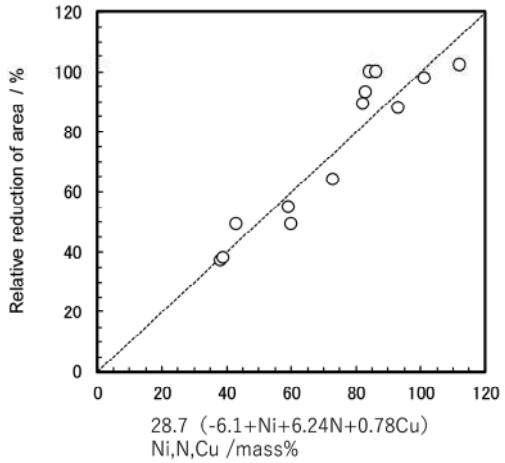

Fig. 5 Multiple regression analysis of relative reduction of area after **SSRT at −40°C by Ni, N and Cu contents**

duced Ni and Mo with Ni equivalent of above 30.2.

The relative reduction of area (relative reduction of area tested in 70 $MPaH_2$ divided by the reduction of area tested in atmospheric air) after SSRT at −40°C was processed by multiple regression analysis with respect to the amounts of Ni, N, Cu, and the effect of the interaction of the added Ni, N, and Cu on the hydrogen gaseous embrittlement was assessed. Figure 5 shows the result of the multiple regression analysis of the relative reduction of area of the 13 steels with respect to the amounts of Ni, N, and Cu. The relationship between the relative reduction of area and the amounts of addition of these elements is as follows, obtained by multiple regression analysis: relative reduction of area=28.7Ni+179N+22.5Cu−173.8= 28.7 (Ni+6.24N+0.78Cu−6.1) (unit of each element: mass%). Coefficients of N and Cu relative to Ni obtained by multiple regression analysis are 6.24 and 0.78, respectively, which generally agree with the coefficients of 7.55 and 0.53 of Sanga's equation, an index of γ phase stability. From this, the hydrogen gaseous embrittlement resistance of the austenitic steel with reduced Ni and Mo has good correlation with γ phase stability, and N and Cu in addition to Ni are considered to be effective elements to enhance hydrogen gaseous embrittlement resistance.

Based on the above results, in the alloy design of STH2, in order to obtain hydrogen gaseous embrittlement resistance at −40°C, N and Cu were added to the basic composition (15Cr-9Mn+Ni) to obtain Ni equivalent equal to or above 30.2 by Sanga's equation.

4. Various Properties of STH2 Steel Sheet

This chapter describes the advantages of various properties of the STH2 steel sheet (Ni equivalent: 30.5) actually produced for testing based on the concept of its alloy design stated in the previous chapter. For the assessment of properties, steel sheet 1.2 mm in thickness and of 2B specification was used.

Figure 6 shows the result of the measurement of 0.2% proof stress and tensile strength. For the measurement, the JIS 13 B tensile test was conducted (L direction) at a strain rate of 8.3×10^{-3}/s (in conformity with JIS Z 2241). In the range of −40 to 100°C, 0.2% proof stress stays within the range of 315 to 490 MPa, the tensile strength stays within the range of 635 to 860 MPa, and the strength of STH2 is 1.2 to 1.5 times higher than that of SUS316L (17.5Cr-12Ni-2Mo). Furthermore, the fracture elongation of STH2 is about 45% at any temperature in the range of −40 to 100°C.

Figure 7 shows stress-elongation curves after SSRT at −40°C in 70 $MPaH_2$. SSRT was conducted at the strain rate of 3×10^{-5}/s for sheet type tensile test pieces (L direction), each having a parallel section of 20 mm in length and a width of 4 mm. STH2 realized high strength of 900 MPa and high ductility fracture elongation of higher than 60%. In comparison with SUS316L, tensile strength increased by 1.3, and fracture elongation increased to the same level. Based on the result of our past research and its mechanism,[17] we consider that the deformation twin (TWIP) of the γ phase also contributes to the high strength and high ductility of STH2 in addition to the rise of the dislocation density by cross-slip at the slow strain rate tension test. Furthermore, the relative fracture strength of STH2 at −40°C, 70 $MPaH_2$ vs. that of SSRT in −40°C atmospheric air (0.1 MPa) was 1.00, and the relative fracture elongation was 0.95. Thus, STH2 has realized high strength and high ductility in SSRT at −40°C in 70 $MPaH_2$, and is equipped with excellent hydrogen gaseous embrittlement resistance.

Figure 8 shows the schematic diagram of the diffusion bonding experiment and observation examples of the microstructures of the bonding interface. Diffusion bonded austenitic stainless steel plates are frequently used for pre-coolers to cool high pressure hydrogen gas.[18] The diffusion bonding experiment was conducted in the following manner. The surfaces of the test samples were miller-finished, heated up to 1 100°C at a heating rate of 300°C per hour in a furnace, and held for three hours under a bearing pressure of 0.5

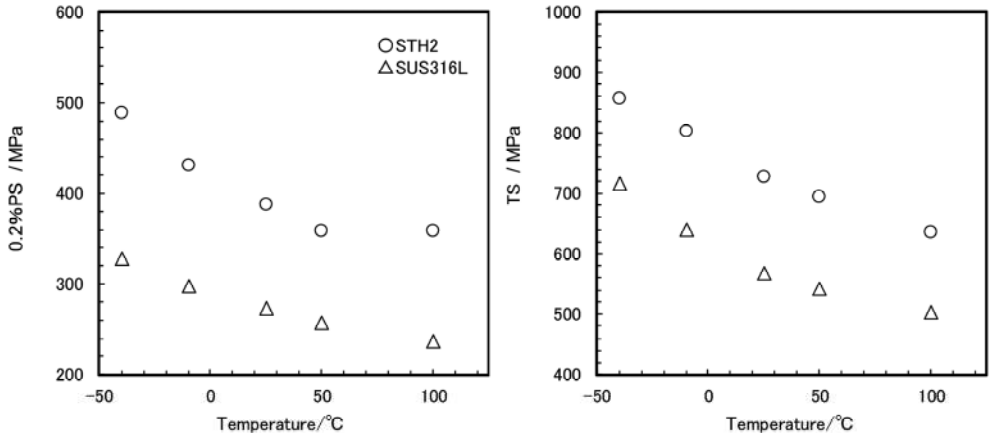

Fig. 6 0.2% proof strength and tensile strength of STH2 and SUS316L

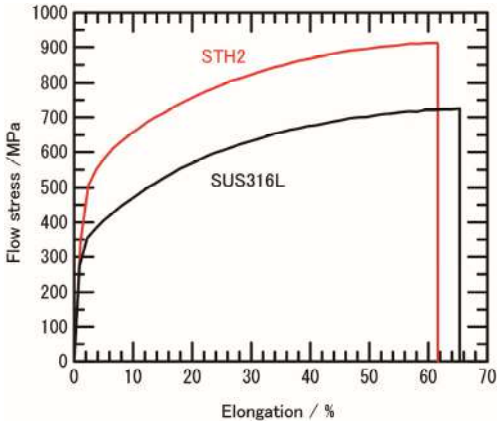

Fig. 7 Stress-elongation curves after SSRT in gaseous hydrogen at 70 MPa at −40°C

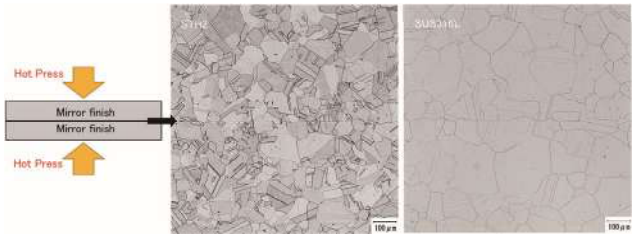

Fig. 8 Schematic diagram of diffusion bonding experiment and optical microscope structure of bonding interface

MPa. The degree of vacuum during holding was 10^{-2} to 10^{-3} Pa. Crystal grains of STH2 and SUS316L were observed across the bonded interface. This observation result showed that the bonded interface has almost disappeared, and STH2 has diffusion bondability almost equal to that of SUS316L.

In **Fig. 9**, examples of observation of the cross section microstructure of TIG-welded material (tungsten inert gas welding) are shown. TIG welding was conducted under the condition that the weld bead is applied in the direction of rolling and the width of the back bead becomes about 2.0 mm (welding current: 200 A, welding speed: 150 cm/min). As the shielding gas, Ar gas was used. In the welds, welding defects such as solidification cracking and/or bubbles were not observed. In addition, the width of the back bead of SUS316L was about 2.0 mm under the same welding condition. Accordingly, STH2 is judged to be TIG-weldable the same as SUS 316L.

Fig. 9 Optical microscope structure of TIG welding material

Fig. 10 Appearance after cyclic corrosion cycle test (JASO, 30 cycles), evaluation surface #600

Figure 10 shows the appearance of the test pieces after a combined cycle test conducted pursuant to the Japanese Automotive Standards Organization (JASO, 30 cycles). One cycle of the test is 8 h and consists of: (1) 5% neutral salt water spray at 35°C for 2 h, (2) dried at 60°C under 25% relative humidity for 4 h, and (3) exposure to moistening atmosphere with a relative humidity of 95% for 2 h. The evaluation surface was #600 wet-polish-finished. The rustiness of STH2 is slight as compared with that of SUS430 (17Cr), and is equivalent to the level of that of the representative austenitic stainless steel SUS304 (18Cr-8Ni).

Table 2 shows the time of the occurrence of stress corrosion cracking (JIS G 0756). The test condition is: U-bent test pieces 75 mm in length and 10 mm in width are immersed in the boiling 42% and 20% $MgCl_2$ solutions for 100 h at the longest. The time of occurrence of stress corrosion cracking of STH2 is comparable to that of SUS304, and stress corrosion cracking resistance of STH2 is al-

Table 2 Time of occurrence of stress corrosion cracking (JIS G 0576 **compliant)**

$MgCl_2$	STH2		SUS304	
	1	2	1	2
20%	○	○	○	○
42%	24 h	24 h	1 h	1 h

○ No cracking after 100 hours

most at the same level as that of SUS304.

Therefore, in comparison with SUS316L, the STH2 steel sheet (Ni equivalent: 30.5) actually produced for the test is compatibly equipped with high strength and applicability to the high pressure hydrogen gaseous environment. STH2 is also equipped with bondability and weather resistance at the same level as those of SUS316L and/or SUS304, and has material properties for application to practical use.

5. Conclusion

This article summarized the result of major research pertaining to the alloy design of austenitic steel with reduced Ni and Mo (STH2) for hydrogen use, and the various properties of the STH2 steel sheet practically produced for the test.

In the alloy design of STH2, to obtain hydrogen gaseous embrittlement resistance at −40°C, Ni equivalent was designed to be equal to or higher than 30.2 (≥30.2) by Sanga's equation by adding N and/or Cu to the basic chemical composition of (15Cr-9Mn+Ni). The effect of adding N and/or Cu on suppressing strain localization in addition to enhancing γ phase stability was revealed. Hydrogen gaseous embrittlement resistance has good correlation with γ phase stability (Sanga's equation), and N and/or Cu in addition to Ni are effective elements for enhancing hydrogen gaseous embrittlement resistance. The STH2 steel sheet practically produced for the test (Ni equivalent: 30.5) is compatibly equipped with high strength and applicability to the high pressure hydrogen gaseous environment. Hereafter, with the promotion of the application of STH2, realization of reduction or effective utilization of rare metals is expected in the future construction of the impending hydrogen energy society.

Acknowledgement

The slow strain rate tension test (SSRT) in the high pressure hydrogen gaseous environment described in Chapter 3 was conducted in the NEDO-sponsored researches of "Development of Technologies for Hydrogen Production, Delivery and Storage Systems" and of "Research and Development on Hydrogen Utilization Technology Research and Development". We wish to express our utmost gratitude to all concerned in the said sponsored research and development.

References

1) NEDO: Establishment of Codes and Standards for Hydrogen Economy Society. 2005−2009 Fiscal Year Report on Result of Research. 2010
2) NEDO: Development of Technologies for Hydrogen Production, Delivery and Storage Systems. 2010−2012 Fiscal Year Report on Result of Research. 2013
3) NEDO: Research and Development on Hydrogen Utilization Technology Research and Development. 2013−2017 Fiscal Year Report on Result of Research. 2018
4) Hatano, M. et al.: Acta Materialia. 67, 342 (2014)
5) Hatano, M. et al.: Philosophical Magazine Letters. 96, 220 (2016)
6) Hatano, M. et al.: Philosophical Magazine Letters. 99, 404 (2019)
7) Yamada, T. et al.: Journal of the High Pressure Gas Safety Institute of Japan. 49 (10), 29 (2012)
8) The High Pressure Gas Safety Institute of Japan: General Gas Security Regulation. 2016
9) Hatano, M. et al.: JRCM NEWS. (375), 2 (2018)
10) Hatano, M. et al.: Forum Symposium of Hydrogen Gaseous Embrittlement Fracture Mechanism and Problem in Application to Actual Use Proceedings, 13, (2019)
11) Imade, M. et al.: CAMP-ISIJ. 20, 1058 (2007)
12) Nakagawa, H. et al.: CAMP-ISIJ. 19, 1160 (2006)
13) Nakagawa, H. et al.: Pressure Vessel and Piping Conference. 26492 (2007)
14) Tsuchita, N. et al.: Journal of the Japan Institute of Metals and Materials. 72 (9), 769 (2008)
15) Ohkubo, N. et al.: ISIJ Int. 34, 764 (1994)
16) Fukuyama, S. et al.: Journal of the Japan Institute of Metals and Materials. 67, 456 (2003)
17) Hatano, M. et al.: Journal of the Japan Institute of Metals and Materials. 77, 593 (2013)
18) Miura, S. et al.: Kobe Steel Eng. Rep. 64 (1), 49 (2014)

Masaharu HATANO
Chief Researcher, Dr. Eng.
Function Creation Research & Development Div.
Research & Development Center
Nippon Steel Stainless Steel Corporation
3434 Ooaza-shimata, Hikari City, Yamaguchi Pref.
743-8550

Kazuhisa MATUMOTO
Manager
Automotive Products Development Gr.
Products Development Div.
Nippon Steel Stainless Steel Corporation

Mitsuki SUGEOI
Researcher
Function Creation Research & Development Div.
Research & Development Center
Nippon Steel Stainless Steel Corporation

Kenji HATTORI
Senior Manager
Coil & Sheet Products Development Gr.
Products Development Div.
Nippon Steel Stainless Steel Corporation